Desalination and Water Treatment
www.deswater.com

doi: 10.1080/19443994.2015.1135084

57 (2016) 22493–22506
October

Taylor & Francis
Taylor & Francis Group

Removal of copper, zinc and cadmium ions through adsorption on water-quenched blast furnace slag

Zhe Wang[a,c], Guohe Huang[a,*], Chunjiang An[a,b], Lirong Chen[c], Jinliang Liu[c]

[a]*MOE Key Laboratory of Regional Energy and Environmental Systems Optimization, Resources and Environmental Research Academy, North China Electric Power University, Beijing 102206, China, Tel. +86 15804721992; email: wz0478@163.com (Z. Wang), Tel. +86 10 61772018; Fax: +86 10 51971284; email: huang@iseis.org (G. Huang), Tel. +86 13063378537; email: chunjiang.an@uregina.ca (C. An)*
[b]*Institute for Energy, Environment and Sustainable Communities, University of Regina, Regina, Saskatchewan S4S 0A2, Canada*
[c]*School of Energy and Environment, Inner Mongolia of Science and Technology, Baotou 014010, China, Tel. +86 18647209636, email: lirc@imust.cn (L. Chen), Tel. +86 15049210362; email: ljliang@126.com (J. Liu)*

Received 8 July 2015; Accepted 2 December 2015

ABSTRACT

Water-quenched blast furnace slag (WBFS) has been assessed regarding its capacity to remove Cu^{2+}, Cd^{2+}, and Zn^{2+} from aqueous solutions. The physicochemical properties of the slag were characterized by ICP, SEM, and XRD. Batch experiments were conducted to study the effects of the adsorbent dosage, pH, initial concentration of heavy metal ions, temperature, and contact time on the removal of Cu^{2+}, Cd^{2+}, and Zn^{2+}. The results showed that the removal efficiency increased with increasing adsorbent dosage and the optimum conditions for the removal of Cu^{2+}, Cd^{2+}, and Zn^{2+} were obtained in the dosage of 12, 16, and 16 g/L, respectively. The removal efficiency and adsorption amount of Cu^{2+}, Cd^{2+}, and Zn^{2+} onto WBFS increased on increasing the solution pH from 1 to 9, while the values decreased slightly as the pH further increased above 9. The adsorption process could fit the pseudo-second-order kinetic and Langmuir isotherm models. Various thermodynamic parameters were calculated and the results indicated the adsorption of Cu^{2+}, Cd^{2+}, and Zn^{2+} onto WBFS was feasible and endothermic in nature. These results have significant implications for the treatment of heavy metal wastewater using low-cost adsorbents.

Keywords: Adsorption; Water-quenched blast furnace slag; Isotherms; Kinetics; Thermodynamics; Heavy metals

1. Introduction

Industrial development is often associated with environmental concerns [1]. Heavy metal contamination has become a major industry-related environmental problem with regard to contamination of water and soil bodies [2]. Particularly, wastewater generated from mining, metallurgical, machinery, chemical, electroplating, and battery-manufacturing industries often contains large amounts of heavy metals such as Cu^{2+}, Cd^{2+}, and Zn^{2+} [3,4]. These toxic heavy metals, especially Cd^{2+}, can cause central nervous system damage in human beings, even at extremely low concentration [5]. Cu^{2+} and Zn^{2+} are essential in small quantities, but they also have adverse effects on human health when exceeding the

*Corresponding author.

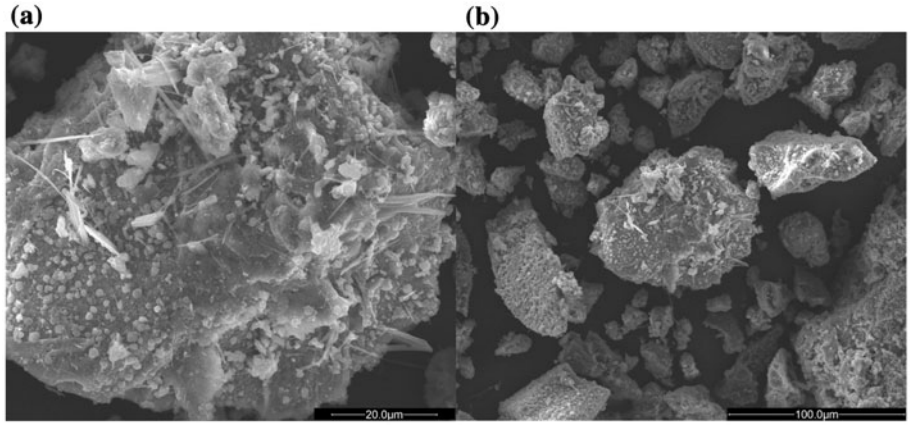

Fig. 1. SEM photographs of WBFS: (a) 20.0 μm and (b) 100.0 μm.

prescribed limit [6,7]. The maximum acceptable concentrations of Cu^{2+}, Zn^{2+}, and Cd^{2+} recommended by the World Health Organization (WHO) for drinking water are less than 2, 3, and 0.003 mg/L, respectively [8]. Moreover, the non-biodegradability of these heavy metals can lead to amplified accumulation of them in natural food chains [9]. Therefore, there has been an increasing need for developing effective strategies to remove heavy metals from contaminated wastewater.

Many techniques such as precipitation, ion exchange, electrochemical treatment, membrane filtration, evaporation, and solidification have been investigated to remove heavy metals from aqueous solution [10]. Some issues including substantial initial capital investment, incomplete metal removal, high maintenance cost, and excess sludge production, however, were addressed in the applications of these treatment techniques [11,12]. As an alternative, adsorption techniques were studied to remove heavy metals from wastewater [13–17]. A number of materials such as silica gel [18,19], activated alumina [20], zeolite, [21] and activated carbon [22–24] were investigated as adsorbents. From the view of economical efficiency and technology sustainability, considerable attention was recently given to the use of low-cost adsorbents in pollution control. The capacities of chitosan [25], clay [26], peat moss [27] and various agricultural wastes [28–30] were evaluated in the treatment of wastewater containing heavy metals. Recently, there was an increasing interest in the utilization of industrial waste as adsorbent. Fly ash was used for removing organic pollutants [31,32], heavy metal ions [33], and phosphate [34] in aqueous phase. However, knowledge about the adsorption of heavy metals on industrial waste adsorbents is still limited.

Large amounts of water-quenched blast furnace slag (WBFS) can be generated during iron-making process, through quick water-cooling of molten substances in iron smelting furnace. WBFS is mainly granular in shape and composed of oxides of calcium, silicon, iron, aluminum, and manganese. The slag has been used as raw material in road construction and inorganic coating, as well as production of slag fiber, wollastonite, and inorganic gel. Previously, the application of furnace slag for the removal of methylene blue dye [35] and As^{3+} was also investigated [36]. However, information about the potential utilization of WBFS as adsorbent for the treatment of heavy metals is unknown. Mechanisms associated with WBFS adsorption characteristics are still limited. Therefore, the objective of this study was to investigate the removal of copper, zinc, and cadmium ions through adsorption on WBFS. Batch experiments will be conducted to evaluate the adsorption performance of WBFS as influenced by initial concentration, pH, contact time, temperature, and adsorbent dosage. The corresponding adsorption isotherms, kinetics, and thermodynamics will be also studied. The results of this study will have important implications for the treatment of heavy metal wastewater using low-cost adsorbents.

2. Materials and methods

2.1. Adsorbent preparation

WBFS samples used in this study were obtained from Baotou Iron and Steel Co., Ltd, Baotou, China. The slags were washed with deionized water to remove surface impurities and dried at 100°C for 24 h. The samples were then crushed, ground, sieved to pass through 100-mesh sieve (0.15 mm), and dried for another 24 h at 105°C. After cooling down to ambient temperature, the WBFS samples were stored in desiccators before use.

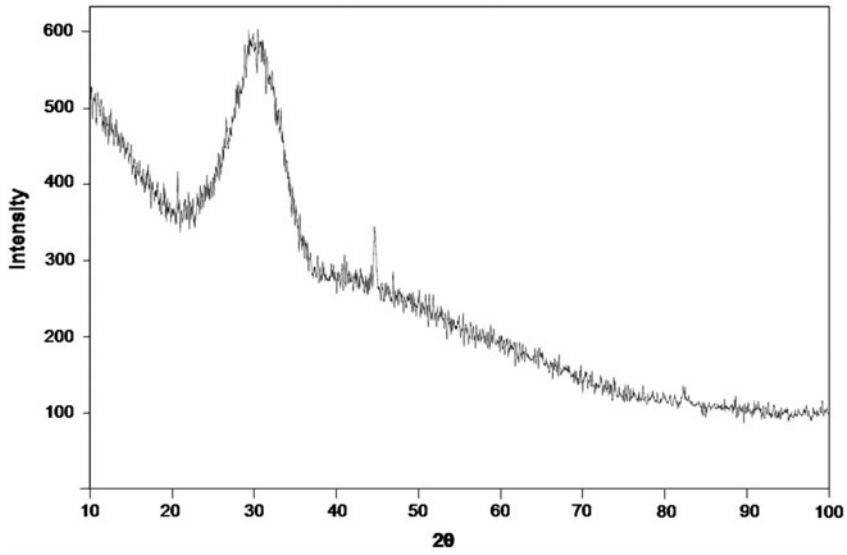

Fig. 2. XRD spectrum of WBFS.

2.2. Chemicals

All chemicals used were of reagent grade quality or higher. $Cu(NO_3)_2{\cdot}3H_2O$, $Cd(NO_3)_2{\cdot}4H_2O$, and $Zn(NO_3)_2{\cdot}6H_2O$ were purchased from Guangyuan Chemical Co., Ltd, in Baotou. Stock solutions of Cu^{2+}, Cd^{2+}, and Zn^{2+} were prepared by dissolving appropriate amount of $Cu(NO_3)_2{\cdot}3H_2O$, $Cd(NO_3)_2{\cdot}4H_2O$, $Zn(NO_3)_2{\cdot}6H_2O$, separately in deionized water. The concentrations of the Cu^{2+}, Cd^{2+}, and Zn^{2+} solutions were in the range of 20–300 mg/L. 1 M-NaOH and 1 M-HCl solutions were used for pH adjustment.

2.3. Analytical methods

Chemical composition of WBFS was analyzed using Inductively Coupled Plasma Mass Spectrometer (ICP-MS, P-5000, Hitachi Corporation, Japan). The surface area of the WBFS was determined from N_2 adsorption by applying the Brunauer–Emmett–Teller (BET) adsorption method using SA3000 apparatus (Beckman Coulter Corporation, USA). A scanning electron microscope (QUANTA400, FEI Corporation, USA) was used for obtaining microscopic images of the WBFS. X-ray diffraction (D8 ADVANCE, Bruker, Germany) was applied to determine the mineral components of the adsorbent. The concentration of metal ions was determined by the atomic absorption spectrometer (AA-6300C, Shimadzu, Japan). The pH level was measured by a pH meter (PHS-3C, Shanghai Precision Scientific Instrument Corporation, China). The compressive strength of concrete was determined by the concrete strength testing instrument (Q61, Shandong Drick Corporation, China).

2.4. Batch adsorption experiments

The batch experiments were carried out in 250-mL conical flasks with stoppers. For each experiment, a specific amount of WBFS was added in 100 mL of Cu^{2+}, Cd^{2+}, and Zn^{2+} solutions at certain concentrations, respectively. Blank experiments were conducted to correct the adsorption by conical flask. All the flasks were placed on a thermo-stated shaker at 120 rpm to reach the adsorption equilibrium. Then, the supernatant was filtered and the concentration of heavy metal ions in the filtrate was determined by the atomic absorption spectrometer. All batch experiments were performed in triplicate and the average data were used in data analysis. The adsorption capacity (mg/g) and removal efficiency (%) were calculated as follows:

$$\text{Adsorption capacity (mg/g)} = ((C_0 - C_e)V)/W \quad (1)$$

$$\text{Removal efficiency (\%)} = (C_0 - C_e) \times 100/C_0 \quad (2)$$

where C_0 (mg/L) and C_e (mg/L) are the initial and equilibrium concentrations of heavy metal ions, respectively. V is the volume of the Cu^{2+}, Cd^{2+}, and Zn^{2+} solution in mL and W is the weight of the adsorbent in g.

2.4.1. Effect of adsorbent dosage

Different amounts of WBFS ranging from 0 to 2.0 g were added to each conical flask to investigate the effect of WBFS dosage on Cu^{2+}, Cd^{2+}, and Zn^{2+}

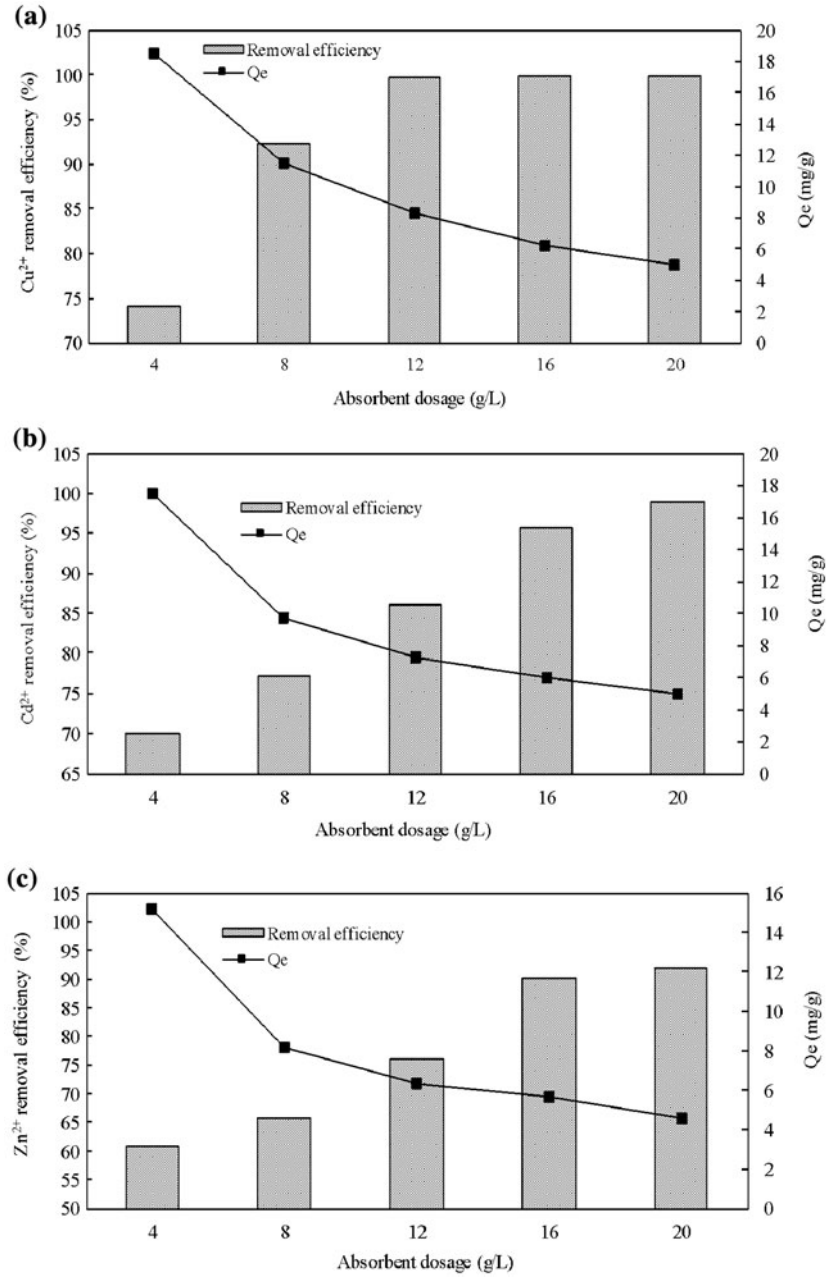

Fig. 3. Effect of adsorbent dosage on the adsorption of (a) Cu^{2+}, (b) Cd^{2+}, and (c) Zn^{2+} onto WBFS.

adsorption. These studies were carried out at pH 7 with a temperature of 25°C. The contact time of 100 min and initial concentrations of 100 mg/L were adopted.

2.4.2. Effect of pH

In order to investigate the effects of pH on heavy metal adsorption by WBFS, solution pH was adjusted to 1–13 through adding appropriate amount of NaOH or HCl. The adsorption of 100 mg/L heavy metals were studied at 25°C after a reaction time of 100 min. The WBFS dosage was 12, 16, and 16 g/L for Cu^{2+}, Cd^{2+}, and Zn^{2+}, respectively.

2.4.3. Adsorption isotherms studies

To better understand the mechanism of adsorption, batch tests were conducted with different initial heavy metal concentrations. The adsorption studies were

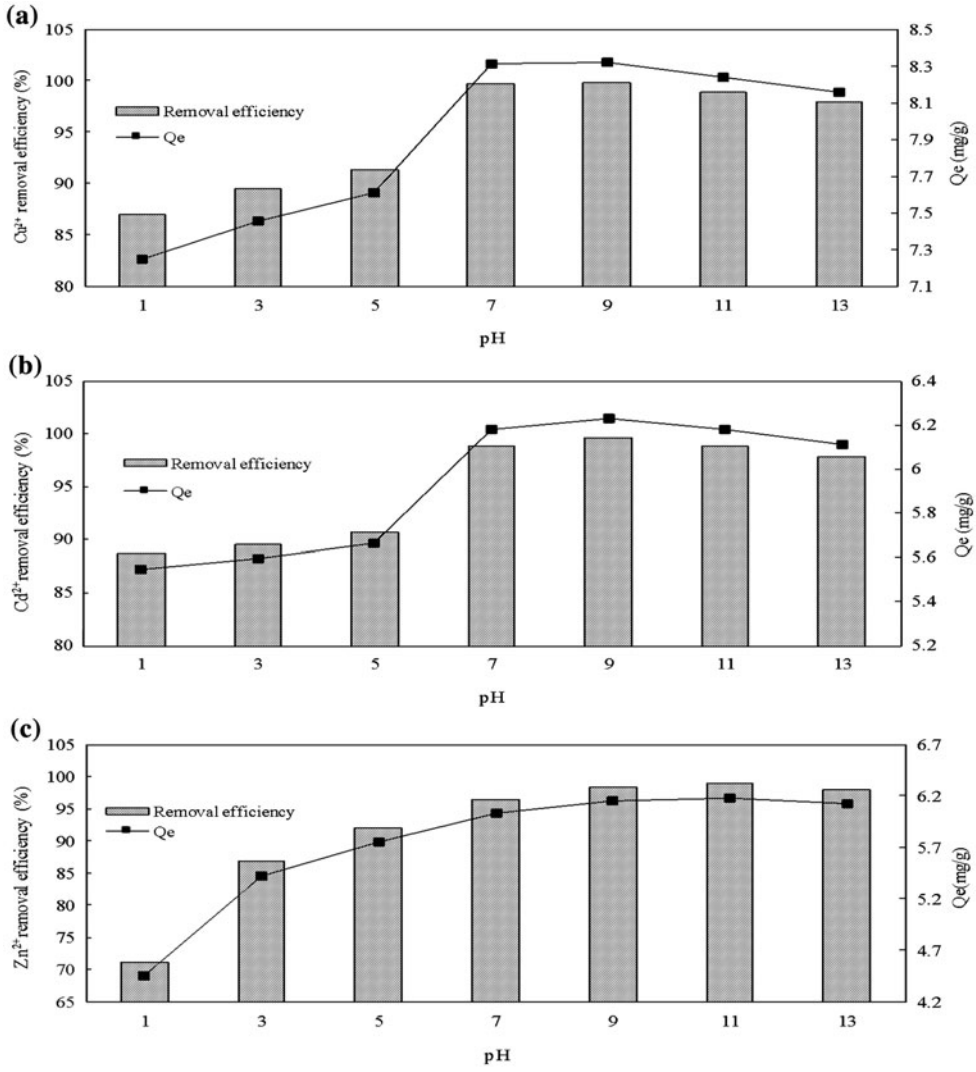

Fig. 4. Effect of pH on the adsorption of (a) Cu^{2+}, (b) Cd^{2+}, and (c) Zn^{2+} onto WBFS.

conducted at fixed adsorbent dosage (12, 16, and 16 g/L for Cu^{2+}, Cd^{2+}, and Zn^{2+}, respectively) by varying initial concentrations of heavy metals from 0 to 300 mg/L at pH 7 and 25˚C. The equilibrium time was 100 min.

2.4.4. Effect of temperature

The relationship between temperature and the adsorption amount of heavy metal ions was investigated. The initial concentration of Cu^{2+}, Cd^{2+}, and Zn^{2+} was 100 mg/L. The WBFS dosage was 12, 16, and 16 g/L for Cu^{2+}, Cd^{2+}, and Zn^{2+}, respectively. The experiments were studied at an agitation time of 100 min at temperatures between 25 and 65˚C at pH 7.

2.4.5. Adsorption kinetics studies

The adsorption kinetics experiments were carried out with initial concentration of 100 mg/L heavy metal ions at pH 7 and 25˚C. Cu^{2+}, Cd^{2+}, and Zn^{2+} solutions were mixed with WBFS at dosage of 12, 16, and 16 g/L, respectively. The concentration of heavy metal ions was monitored at different time intervals, ranging from 20 to 100 min.

3. Results and discussion

3.1. Physicochemical characterization of WBFS

The adsorption process at the interface between liquid phase and solid phase can be often influenced by adsorbent characteristics. To reveal the mechanism

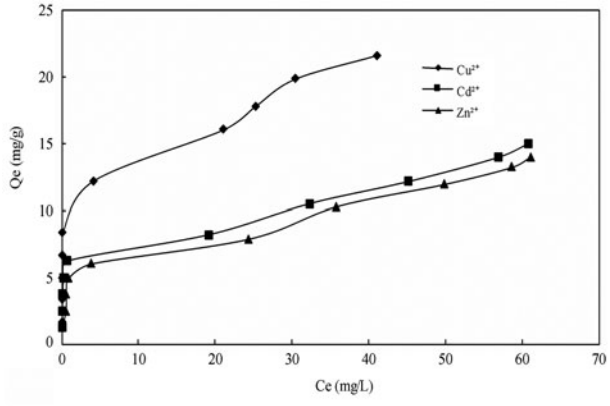

Fig. 5. Adsorption isotherms of Cu^{2+}, Cd^{2+}, and Zn^{2+} onto WBFS.

of adsorption of heavy metal ions on WBFS, the physicochemical properties of WBFS need to be determined at first. The properties and major chemical constituents of WBFS are presented in Table 1. It can be seen that WBFS mainly consist of CaO and SiO_2 (more than 66% by mass). This is similar to the composition of steel-making slag [37]. SiO_2 exists in the form of $(SiO_4)^{4-}$ when the WBFS are put into solution. $(SiO_4)^{4-}$ belong to the crystal structure, which can promote ion exchange and adsorption [38]. In addition, the total content of oxide in WBFS is high, which can reflect strong affinity for heavy metals [39]. Therefore, the WBFS is expected to be an adsorbent for heavy metal ions. The SEM micrographs of WBFS are shown in Fig. 1. The coarse, loose, and porous surface textures of WBFS samples were observed. The slag particles had subrounded to angular shapes and distinct asperities and edges were visible. They were also characterized by rough surface textures. The XRD pattern of WBFS is shown in Fig. 2. The XRD patterns of the WBFS samples were very complex which were mainly attributed to the raw material composition. The XRD results showed the sample could be vitreous with an amorphous hump of the glass around 28° 2θ [40]. During the formation of WBFS, rapid quenching can prevent the formation of complete crystal structures. It should be also noted several peaks were observed. It indicated the crystal phase was also present in the slag.

Table 1
Properties and major chemical constituents of WBFS

Properties	Descriptions
CaO (%)	33.60
SiO_2 (%)	32.99
Al_2O_3 (%)	12.46
MgO (%)	10.45
Fe_2O_3 (%)	0.86
ThO_2 (%)	0.02
BET surface area (m^2/g)	3.83
Density (g/cm^3)	2.71

3.2. Effect of WBFS dosage

Effect of WBFS dosage on the removal of Cu^{2+}, Cd^{2+}, and Zn^{2+} was investigated and the results are presented in Fig. 3. When the adsorbent dosage was less than 12 g/L, the removal efficiency of Cu^{2+} on WBFS increased rapidly as the adsorbent dosage increased. However, when the WBFS dosage was higher than 12 g/L, there was slow rise as the WBFS dosage further increased. With the WBFS dosage increasing from 16 to 20 g/L, the Cu^{2+} removal efficiency increased from 99.85 to 99.89%, while the adsorbed amount of Cu^{2+} decreased from 6.24 to 4.99 mg/g. For the adsorbent dosage of 16 g/L, the removal efficiency and the adsorbed amount of Cd^{2+} were 95.76% and 5.99 mg/g, respectively. When the adsorbent dosage increased to 20 g/L, the removal efficiency increased by 3.15%, the adsorption amount decreased by 17.53%. As for Zn^{2+}, the removal efficiency increased gradually, along with the increasing dosage of WBFS. After the dosage increased above 16 g/L, removal efficiency would not significantly increase. 12, 16, and 16 g/L were considered as the optimum dosages for the removal of Cu^{2+}, Cd^{2+}, and Zn^{2+} by WBFS, respectively.

In general, the removal efficiency trend was almost the same for the three heavy metal ions tested in this study. The removal efficiency increased with increase in the amount of adsorbent dosage within a certain range, and thereafter there was no significant change in removal efficiency. However, the adsorbed amount of Cu^{2+}, Cd^{2+}, and Zn^{2+} continued to decrease. This may be explained by the increased surface area and the corresponding increase in the surface active sites available for adsorption, resulting in decreasing adsorption amount per unit mass [41]. This result confirms the previous studies concerning the removal of Cd(II) from acidic aqueous solution by modified steel-making slag [42]. In addition, at the same dosage value, the removal efficiency sequence was $Cu^{2+} > Cd^{2+} > Zn^{2+}$. It showed that the adsorption of these three kinds of heavy metal ions was selective. This could be attributed to the difference in adsorbent structure, radius, and free energy of the hydrated ions [43].

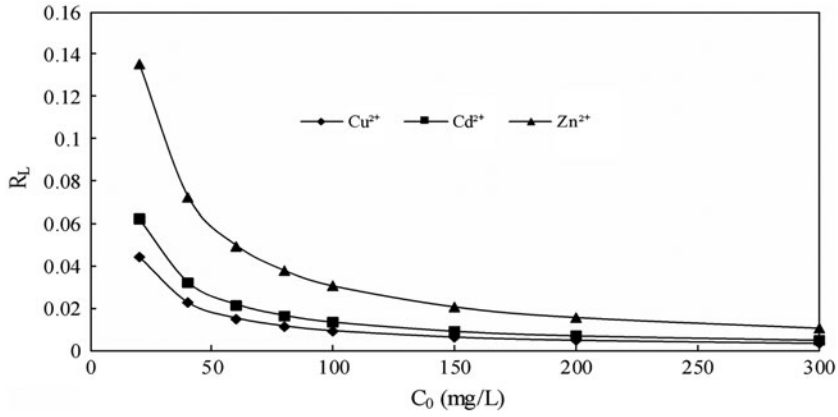

Fig. 6. Varying R_L values associated with the adsorption of Cu^{2+}, Cd^{2+}, and Zn^{2+} onto WBFS.

3.3. Effect of pH

The pH of aqueous solution is an important factor for controlling adsorption process. The effect of pH on adsorption of Cu^{2+}, Cd^{2+}, and Zn^{2+} by WBFS was studied and the results are shown in Fig. 4. The removal efficiency and adsorption amount of Cu^{2+}, Cd^{2+}, and Zn^{2+} increased when pH varied from 1 to 9. When the pH was above 9, the values decreased slightly. The removal efficiency of Cu^{2+} increased slowly at pH lower than 5. The removal efficiency and adsorption amount of Cu^{2+} at pH 5 were 91.29% and 7.61 mg/g, respectively. After that, with the increase of pH in solution, $Cu(OH)_2$ was produced. This resulted in Cu^{2+} removal efficiency up to 99.7% and the adsorption amount of Cu^{2+} up to 8.31 mg/g at pH 7. The variation trend of Cd^{2+} influenced by pH was similar with that of Cu^{2+}. As for Zn^{2+}, the removal efficiency increased rapidly from 71.06% to 86.74% at $pH < 3$, followed by a gradual rise at $pH > 3$. Thereafter, the precipitation of $Zn(OH)_2$ was produced as pH further increased, the maximum removal efficiency of 98.84% and adsorption amount of 6.18 mg/g were observed at pH 11. Therefore, pH 7 was considered as optimum condition and was used for further study.

The heavy metals in solution exist in cationic state at low pH. High-concentration H^+ present in the reaction solutions can compete with heavy metal ions for the adsorption sites [44]. Hence, the adsorption capability of heavy metals on WBFS surface was poor in a low pH. With an increase in pH, the competing effect of H^+ ions decreased and the heavy metals still existed in the form of ionic state. The adsorption of heavy metals through ion exchange was mainly embodied at this time. As the solution pH further increased, the binding of ionic state of heavy metals to OH^- ions could form substances of limited solubility, so it is advantageous to combine. There would be complex adsorption on the surface of adsorbent and heavy metal ions in solution can be transformed from ionic status to insoluble hydroxides [45]. At the same time, the WBFS adsorbent not only plays a role in the exchange adsorption, but also in crystal seeding for heavy metal ions. This will be favorable for the precipitation of hydroxides and can lead to co-precipitation during the settlement process, resulting in a higher efficiency for the removal of heavy metal ions. The crystal seeding of adsorbent was enhanced and the exchange adsorption capacity weakened when pH further increased, due to the precipitation of hydroxides of heavy metal ions.

3.4. Adsorption isotherms

Fig. 5 shows the adsorption isotherms of Cu^{2+}, Cd^{2+}, and Zn^{2+} on WBFS at 25°C. The adsorption amount showed a fast ascending trend at the initial stage, followed by a gradual rise with different equilibrium solute concentrations for these heavy metals. WBFS exhibited a strong affinity for these three kinds of heavy metal ions, leading to a high adsorption efficiency and low residual amount of heavy metal ions in solution. The heavy metal ions were almost completely absorbed, even in very low concentration. The experimental adsorption data was fit to the Langmuir, Freundlich, Dubinin–Redushckevich (D–R), and Tempkin models as follows to interpret the possible adsorption mechanisms.

Langmuir isotherm:

$$\frac{C_e}{Q_e} = \frac{1}{Q_m} C_e + \frac{1}{K_L \cdot Q_m} \tag{3}$$

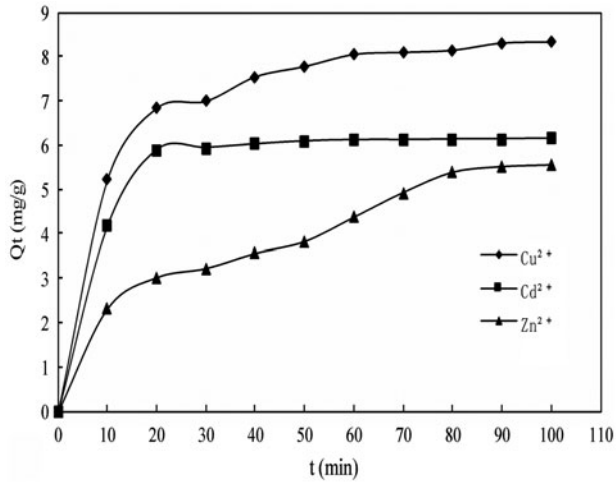

Fig. 7. Adsorption kinetic curves of Cu^{2+}, Cd^{2+}, and Zn^{2+} onto WBFS.

Freundlich isotherm:

$$\ln Q_e = \ln K_F + \left(\frac{1}{n}\right) \ln C_e \quad (4)$$

D–R isotherm:

$$\ln Q_e = \ln Q_m - k\varepsilon^2 \quad (5)$$

$$\varepsilon = RT \ln\left(1 + \frac{1}{C_e}\right) \quad (6)$$

$$E = -\frac{1}{\sqrt{2k}} \quad (7)$$

Tempkin isotherm:

$$Q_e = B \ln A + B \ln C_e \quad (8)$$

where Q_e is the amount of heavy metal ions adsorbed at equilibrium (mg/g); C_e is the equilibrium concentration in solution (mg/L); Q_m is the maximum adsorptive capacity (mg/g); K_L is the Langmuir constant of adsorption (L/mg) and related to the free energy of adsorption [46]; K_F (mg/g) and n are Freundlich constants, K_F is the adsorption capacity of adsorbent and n is the intensity of adsorption [47]; k is a constant related to the adsorption energy (mol^2/kJ^2), ε is the Polanyi potential (J/mol), R is the gas constant (8.314 J/(mol K)), T is absolute temperatures (K), and E is the mean free energy of adsorption, when $|E| < 8$ kJ/mol, the mechanism is physical adsorption, when $8 < |E| < 16$ kJ/mol, the adsorption process is triggered by iron exchange, $|E| > 16$ kJ/mol, the adsorption process is of a chemical nature [48]; A and B are the Temkin constants. The Langmuir model is usually applied for homogeneous surfaces. It assumes the absence of interaction between the different adsorbed molecules and the adsorption with an ideal monolayer formation [49], whereas the Freundlich isotherm model predicts non-ideal sorption on heterogeneous surfaces with multilayer sorption. The D–R isotherm model can be used to calculate the free energy of adsorption, based on micropore filling mechanism on the uniform surface of energy distribution [50]. Tempkin model considers the effects of some indirect adsorbate/adsorbent interactions and suggests that the adsorption heat for all molecules in the layer will decrease linearly with coverage of molecules [51]. The related parameters of these models are listed in Table 2.

When comparing the correlation coefficients, the Langmuir isotherm model ($0.9859 < R^2 < 0.9915$) showed a better fit to the experimental data than the other isotherm models. This indicated the adsorption process of three heavy metal ions on the WBFS could include a monolayer adsorption within the concentration range of 20–300 mg/L. This conclusion was similar to the results of some previous studies [52,53]. The constant K_L can reflect the adsorption ability of adsorbent in the Langmuir model. The K_L constants of three

Table 2
Adsorption parameters for different heavy metals

	Cu^{2+}	Cd^{2+}	Zn^{2+}
Langmuir model			
Q_m (mg/g)	21.32	13.30	14.86
K_L (L/mg)	1.09	0.76	0.32
R^2	0.9915	0.9888	0.9859
Freundlich model			
K_F (mg/g)	8.16	4.98	3.65
n	3.80	4.05	3.18
R^2	0.7897	0.8244	0.9350
D–R model			
Q_m (mg/g)	40.56	25.19	25.13
k (mol^2/kJ^2)	0.0020	0.0018	0.0025
E (kJ/mol)	−15.82	−16.67	−14.14
R^2	0.8180	0.8508	0.9486
Tempkin model			
A (L/mg)	103.87	82.74	17.77
B	2.26	1.45	1.62
R^2	0.9183	0.8915	0.8802

heavy metal ions decreased in the order of $Cu^{2+} > Cd^{2+} > Zn^{2+}$, suggesting that the adsorption ability of the WBFS for Cu^{2+} was higher than those for Cd^{2+} and Zn^{2+}. The results showed the theoretical maximum adsorptive capacities of Cu^{2+}, Cd^{2+}, and Zn^{2+} were 21.32, 13.30, and 14.86 mg/g, respectively.

The basic characteristics of the Langmuir model can be expressed in terms of a dimensionless constant R_L [54], which is defined as Eq. (9):

$$R_L = \frac{1}{1 + K_L C_0} \tag{9}$$

where C_0 is the initial heavy metal ion concentration (mg/L), K_L is the Langmuir constant. The value of R_L indicates the feasibility of the adsorption process. The process is irreversible if $R_L = 0$, favorable if $R_L < 1$, linear if $R_L = 1$, and unfavorable if $R_L > 1$. The results are shown in Fig. 6. The R_L values associated with the initial concentration were found to be between 0 and 1 for all three heavy metal ions at different concentrations. It indicated a favorable adsorption of Cu^{2+}, Cd^{2+}, and Zn^{2+} on the WBFS. The adsorption on WBFS was suitable for wastewater containing low-concentration heavy metals due to the low initial concentration along with a high R_L value.

It has been reported that n is a parameter related to the intensity of adsorption in the Freundlich model. n in the range of 1–10 can indicate favorable adsorption [55]. From the result of Table 2, it could also confirm that the adsorption processes of Cu^{2+}, Cd^{2+} and Zn^{2+} on the WBFS were all favorable. The maximum adsorptive capacity calculated by D–R model was much greater than the values of Langmuir model, which were inconsistent with the experimental results. The assumption of D–R model all micropores are filled with solute, could be an ideal state and might be not applicable in the adsorption on WBFS. The $|E|$ values of Cu^{2+} and Zn^{2+} were between 8.0 and 16.0 kJ /mol, indicating the adsorption process through ion exchange; the $|E|$ of Cd^{2+} was larger than 16 kJ /mol, implying a chemical sorption in this process. The R^2 values of Temkin isotherm were between 0.8802 and 0.9183, which suggested the adsorption heat changed linearly as temperature changed.

3.5. Adsorption thermodynamics

Based on the basic concepts of thermodynamics, the energy of the system is constant, and it can neither be gained nor lost. Entropy is the driving force of change assuming the existence of an isolated system [56]. In order to determine the effect of temperature on the adsorption process, thermodynamic parameters such as change in standard free energy (ΔG), enthalpy (ΔH), and entropy (ΔS) was calculated using the following equations [57]:

$$\Delta G = -RT \ln K_c \tag{10}$$

$$\Delta G = \Delta H - T\Delta S \tag{11}$$

where K_c is the distribution coefficient of the solution between the adsorbent and the solution in equilibrium (Q_e/C_e) [58], R is the gas constant (8.314 J/(mol K)), and T is absolute temperatures (K). The enthalpy (ΔH) and entropy (ΔS) were determined using van't Hoff equation:

$$\ln(K_c) = \frac{\Delta S}{R} - \frac{\Delta H}{RT} \tag{12}$$

The calculated thermodynamic parameters are presented in Table 3. It showed that the equilibrium distribution constant K_c increased with increasing temperatures. Higher K_c showed more heavy metal ions were removed by adsorption on WBFS. This may be attributed to the enhancement of Cu^{2+}, Cd^{2+}, and Zn^{2+} mobility in solution with increasing temperatures, which is helpful to overcome the steric hindrance and accelerate the adsorption [59]. The ΔG values for the adsorption of Cu^{2+} and Cd^{2+} were negative at all temperatures, indicating that the adsorption process was spontaneous. Negative ΔG values were obtained only at temperature higher than 318 K for Zn^{2+} adsorption. The values of ΔG decreased with increasing temperature. This suggested that an increasing trend in the degree of spontaneity and feasibility of Cu^{2+}, Cd^{2+}, and Zn^{2+} adsorption. The ΔH values were calculated to be 17.03, 68.99, and 52.45 kJ/mol for Cu^{2+}, Cd^{2+}, and Zn^{2+}, respectively. The positive ΔH value suggests the endothermic nature of the adsorption process. The ΔS value was found to be 82.33, 243.32, and 167.52 J/mol K for Cu^{2+}, Cd^{2+}, and Zn^{2+}, respectively. The positive values of ΔS imply an increasing disorder at solid/solution interface during the adsorption process.

3.6. Adsorption kinetics

Kinetic studies were performed to investigate the effect of contact time on Cu^{2+}, Cd^{2+}, and Zn^{2+} adsorption by WBFS. The adsorbed amount of heavy metal ions is shown in Fig. 7. The results indicated that the adsorption amount of Cu^{2+}, Cd^{2+}, and Zn^{2+} on WBFS reached a relatively high level within 20 min, and then

Table 3
The thermodynamic parameters for adsorption of Cu^{2+}, Cd^{2+}, and Zn^{2+}

Heavy metal ions	Temperature (K)	ln K_c	ΔG (kJ/mol)	ΔH (kJ/mol)	ΔS (J/mol K)
Cu^{2+}	298	2.96	−7.34	17.03	82.33
	308	3.21	−8.23		
	318	3.65	−9.64		
	328	3.69	−10.07		
	338	3.73	−10.48		
Cd^{2+}	298	1.52	−3.77	68.99	243.32
	308	2.29	−5.88		
	318	2.32	−6.15		
	328	4.08	−11.11		
	338	4.78	−13.43		
Zn^{2+}	298	−1.01	2.50	52.45	167.52
	308	−0.02	0.06		
	318	0.01	−0.03		
	328	0.50	−1.37		
	338	1.88	−5.28		

slowly increased until it reaches an equilibrium concentration.

Some kinetic models can be used to investigate the dynamic adsorption process. The pseudo-first-order and pseudo-second-order models are used to investigate the mechanism of adsorption and potential rate controlling steps such as chemical reaction, diffusion control, and mass transport process. The adsorption mechanism of adsorbate onto adsorbent may be assumed to involve one or more steps. Generally, in a batch reactor intraparticle diffusion is often rate-limiting. To better understand the adsorption process, intraparticle diffusion equation can be also used to analyze the data.

The Lagergren pseudo-first-order model [60] was given by Eq. (13):

$$\ln(Q_e - Q_t) = \ln Q_e - k_1 t \tag{13}$$

where k_1 (1/min) is the first-order rate constant, Q_t and Q_e are the amounts of Cu^{2+}, Cd^{2+}, and Zn^{2+} adsorbed (mg/g) at time t (min) and at equilibrium, respectively. The values of k_1 and Q_e were calculated from the slope and the intercept of the plots of ln $(Q_e - Q_t)$ vs. t, respectively.

The pseudo-second-order model [61] was expressed by Eq. (14):

$$\frac{t}{Q_t} = \left(\frac{1}{k_2 Q_e^2}\right) + \left(\frac{t}{Q_e}\right) \tag{14}$$

where k_2 (g(min mg)) is the second-order rate constant of adsorption. The values of k_2 and Q_e were calculated from the plots of t/Q_t vs. t. Additionally, the initial adsorption rate, h (mg/(g min)) can be determined from K_2 and Q_e values using $h = k_2 Q_e^2$.

The intraparticle diffusion model [62] was given by Eq. (15):

$$Q_t = k_i t^{0.5} + C \tag{15}$$

where k_i is the rate constant of the intraparticle diffusion. C is the intercept which represented the extent of boundary layer thickness. The values of k_i and C were calculated from the plots of Q_t vs. $t^{0.5}$.

The calculated parameters of these kinetic models are listed in Table 4. The results indicated the pseudo-second-order kinetics equation exhibited higher correlation coefficient, and the theoretical $Q_{e,cal}$ values obtained from the pseudo-second-order kinetics model were close to the experimental $Q_{e,exp}$ values. The pseudo-second-order model did not rely on equilibrium adsorption capacity which was usually difficult to be determined accurately by experiments. The second-order model could be used to favorably explain the Cu^{2+}, Cd^{2+}, and Zn^{2+} adsorption on WBFS, which suggested that the process controlling the rate may be chemical sorption. However, the result was not in good agreement with the predictions of D–R isotherm model. As for Cu^{2+} and Zn^{2+}, this could be due to the result of joint action by chemical adsorption and ion exchange adsorption. The h and K_2 values calculated

Table 4
Kinetic parameters for adsorption of Cu^{2+}, Cd^{2+}, and Zn^{2+} onto WBFS

Kinetic model	Parameters	Cu^{2+}	Cd^{2+}	Zn^{2+}
Pseudo-first-order	$Q_{e,exp}$ (mg/g)	8.52	6.18	6.54
	$Q_{e,cal}$ (mg/g)	2.72	0.44	5.44
	K_1 (1/min)	0.0261	0.0258	0.0173
	R^2	0.9818	0.9607	0.9551
Pseudo-second-order	$Q_{e,exp}$ (mg/g)	8.52	6.18	6.54
	$Q_{e,cal}$ (mg/g)	8.81	6.22	7.55
	K_2 (g/(mg min))	0.0185	0.1365	0.0035
	h (mg/(g min))	1.4359	5.2810	0.1995
	R^2	0.9998	0.9999	0.9635
Intraparticle diffusion	C	5.7618	5.7031	0.6414
	k_i (mg/(g $min^{0.5}$))	0.2684	0.0469	0.4973
	R^2	0.9442	0.9203	0.9478

from the pseudo-second-order kinetic model were higher for Cd^{2+} than those for Cu^{2+} and Zn^{2+}, indicating that Cd^{2+} showed faster adsorption kinetics than Cu^{2+} and Zn^{2+}. Similar results were also observed when Li et al. [63] studied the adsorption of Cu^{2+}, Pb^{2+}, Zn^{2+}, and Cd^{2+} on poly (vinyl alcohol)/chitosan beads.

There are three stages in the adsorption process, including external surface adsorption stage, intraparticle diffusion stage, and the final equilibrium stage [64]. To better understand the diffusion mechanisms, the intraparticle diffusion model was also used in data analysis. The correlation coefficients lower than 0.95 were obtained when the data were fit to intraparticle diffusion model. The results suggested that the intraparticle diffusion model was not suitable for the adsorption of Cu^{2+}, Cd^{2+}, and Zn^{2+}. This indicated that the adsorption of heavy metal ions was not dominated by intraparticle diffusion inside the micropores.

3.7. Reutilization of WBFS after adsorption

Inappropriate disposal of adsorbents after wastewater treatment may lead to secondary pollution. In the present study, the used WBFS after adsorption was mixed with standard sand and cement clinker in a blender (the percentage of WBFS was 20%) according to "The National Standard of Ready Mixed Concrete" (GBT14902–2012) [65]. The mixtures were placed in the moisture- and temperature-controlled chamber of vibration molding machine. The temperature was kept at 20 ± 2℃ and relative humidity was not less than 50%. Then the mixtures were placed in cement concrete standard curing box at 20 ± 1℃. After 3, 28,' and 60 d, the specimens were tested for their compressive strength levels. The results showed that the samples had a compressive strength of 36.0, 42.7, and 55.8 MPa for the samples after 3, 28, and 60 d, respectively, which met the national standard for P.042.5 ordinary Portland cement. The technology of using recycled WBFS as the component of confect concrete can not only help resolve the potential secondary pollution issue, but also provide a further economic benefit. Therefore, the application of WBFS in wastewater treatment can be featured by its economic efficiency and environmental sustainability.

4. Conclusions

This study presented the performance of WBFS for removing target pollutant Cu^{2+}, Cd^{2+}, and Zn^{2+} from aqueous solution. The results showed the removal efficiencies increased with increasing WBFS dosage. The solution pH was also an important factor for the removal of heavy metal ions. Langmuir isotherm model can be used to well describe the adsorption isotherms, suggesting that heavy metal ions perform as a single molecule layer for WBFS adsorption. The change of heavy metal adsorption with time showed a two-step characteristic. The adsorption followed pseudo-second-order kinetics, which suggested that the process controlling the rate could be a chemical sorption between adsorbent and metal ions. The thermodynamic results indicated that adsorption of Cu^{2+} and Cd^{2+} onto WBFS was spontaneous, while negative ΔG values were obtained only at temperatures higher than 318 K for Zn^{2+} adsorption. The positive ΔH value suggests the endothermic nature of the adsorption

process. The positive values of ΔS implied that the system disorder increased in the duration.

The experimental results presented the potential of WBFS as a low-cost adsorbent for the removal of Cu^{2+}, Cd^{2+}, and Zn^{2+} pollutants from industrial wastewater. The removal efficiency through adsorption on WBFS can be also influenced by aqueous chemistry in the system. The results can help understand the migration patterns of heavy metals in solid–liquid interface. The influencing parameters gained from the current study can be used for the design and optimization of pilot treatment system. Further study is also needed to help obtain more theoretical foundation for the interactions of heavy metal pollutant and WBFS characteristics. Different WBFS types and optimal design for treatment system will be also investigated for scale-up application.

Acknowledgments

This research was supported by the MOE Key Project Program (311013), the Program for Innovative Research Team in University (IRT1127), and the National Natural Science Foundation of China (No. 51190095 and No. 51309096). We are thankful to Baotou Iron and Steel Co., Ltd, for providing the WBFS samples. The authors are also grateful to the editors and the anonymous reviewers for their insightful comments and suggestions.

References

[1] Q. Hu, G.H. Huang, Y.P. Cai, W. Sun, Planning of electric power generation systems under multiple uncertainties and constraint-violation levels, J. Environ. Inf. 23(1) (2014) 55–64.
[2] L. Cutillas-Barreiro, L. Ansias-Manso, D. Fernández-Calviño, M. Arias-Estévez, J.C. Nóvoa-Muñoz, M.J. Fernández-Sanjurjo, E. Álvarez-Rodríguez, A. Núñez-Delgado, Pine bark as bio-adsorbent for Cd, Cu, Ni, Pb and Zn: Batch-type and stirred flow chamber experiments, J. Environ. Manage. 144 (2014) 258–264.
[3] T. Lee, Removal of heavy metals in storm water runoff using porous vermiculite expanded by microwave preparation, Water, Air, Soil Pollut. 223 (2012) 3399–3408.
[4] S. Megateli, S. Semsari, M. Couderchet, Toxicity and removal of heavy metals (cadmium, copper, and zinc) by *Lemna gibba*, Ecotoxicol. Environ. Saf. 72 (2009) 1774–1780.
[5] D. Mohan, K.P. Singh, Single- and multi-component adsorption of cadmium and zinc using activated carbon derived from bagasse-an agricultural waste, Water Res. 36 (2002) 2304–2318.
[6] C.M. Futalan, C.C. Kan, M.L. Dalida, K.J. Hsien, C. Pascua, M.W. Wan, Comparative and competitive adsorption of copper, lead, and nickel using chitosan immobilized on bentonite, Carbohydr. Polym. 83 (2011) 528–536.
[7] P.C. Mishra, R.K. Patel, Removal of lead and zinc ions from water by low cost adsorbents, J. Hazard. Mater. 168 (2009) 319–325.
[8] Available from: <http://www.who.int/watersanitationhealth/dwq/gdwq3rev/en/index.html>.
[9] A.P. Lim, A.Z. Aris, A review on economically adsorbents on heavy metals removal in water and wastewater, Rev. Environ. Sci. Biotechnol. 13 (2014) 163–181.
[10] A. Bhatnagar, F. Kaczala, W. Hogland, M. Marques, C.A. Paraskeva, V.G. Papadakis, M. Sillanpää, Valorization of solid waste products from olive oil industry as potential adsorbents for water pollution control—A review, Environ. Sci. Pollut. Res. 21 (2014) 268–298.
[11] Z. Aksu, F. Gönen, Z. Demircan, Biosorption of chromium(VI) ions by Mowital®B30H resin immobilized activated sludge in a packed bed: Comparison with granular activated carbon, Process Biochem. 38 (2002) 175–186.
[12] W. Zheng, X.M. Li, F. Wang, Q. Yang, P. Deng, G.M. Zeng, Adsorption removal of cadmium and copper from aqueous solution by areca: A food waste, J. Hazard. Mater. 157 (2008) 490–495.
[13] S. Babel, T.A. Kurniawan, Low-cost adsorbents for heavy metals uptake from contaminated water: A review, J. Hazard. Mater. 97 (2003) 219–243.
[14] W. Chouyyok, Y. Shin, J. Davidson, W.D. Samuels, N.H. LaFemina, R.D. Rutledge, G.E. Fryxell, T. Sangvanich, W. Yantasee, Selective removal of copper(II) from natural waters by nanoporous sorbents functionalized with chelating diamines, Environ. Sci. Technol. 44 (2010) 6390–6395.
[15] S.S. Lee, K.L. Nagy, C. Park, P. Fenter, Heavy metal sorption at the muscovite (001)–fulvic acid interface, Environ. Sci. Technol. 45 (2011) 9574–9581.
[16] N. Rahman, U. Haseen, Equilibrium modeling, kinetic, and thermodynamic studies on adsorption of Pb(II) by a hybrid inorganic-organic material: Polyacrylarnide zirconium(IV) iodate, Ind. Eng. Chem. Res. 53 (2014) 8198–8207.
[17] S.J. Lee, J.H. Park, Y.T. Ahn, J.W. Chung, Comparison of heavy metal adsorption by peat moss and peat moss-derived biochar produced under different carbonization conditions, Water Air Soil Poll. 226 (2015) 1–11.
[18] A. Çimen, M. Torun, A. Bilgiç, Immobilization of 4-amino-2-hydroxyacetophenone onto silica gel surface and sorption studies of Cu(II), Ni(II), and Co(II) ions, Desalin. Water Treat. 53 (2015) 2106–2116.
[19] X. Wang, Y. Pei, M. Lu, X. Lu, X. Du, Highly efficient adsorption of heavy metals from wastewaters by graphene oxide-ordered mesoporous silica materials, J. Mater. Sci. 50 (2015) 2113–2121.
[20] M.U. Khobragade, A. Pal, Adsorptive removal of Cu(II) and Ni(II) from single-metal, binary-metal, and industrial wastewater systems by surfactant-modified alumina, J. Environ. Sci. Health, Part A 50 (2015) 385–395.
[21] T. Motsi, N.A. Rowson, M.J.H. Simmons, Adsorption of heavy metals from acid mine drainage by natural zeolite, Int. J. Miner. Process. 92 (2009) 42–48.
[22] C. Gabaldón, P. Marzal, A. Seco, J.A. Gonzalez, Cadmium and copper removal by a granular activated carbon in laboratory column systems, Sep. Sci. Technol. 35 (2000) 1039–1053.

[23] L.F. Yang, Z. Shi, Enhanced electrosorption capacity for lead ion removal with polypyrrole and air-plasma activated carbon nanotube composite electrode, J. Appl. Polym. Sci. 132 (2015) 1–7.
[24] T.M. Alslaibi, I. Abustan, M.A. Ahmad, A. Abu Foul, Comparative studies on the olive stone activated carbon adsorption of Zn^{2+}, Ni^{2+}, and Cd^{2+} from synthetic wastewater, Desalin. Water Treat. 54 (2015) 166–177.
[25] X.Y. Li, H.H. Zhou, W.Q. Wu, S.D. Wei, Y. Xu, Y.F. Kuang, Studies of heavy metal ion adsorption on Chitosan/Sulfydryl-functionalized graphene oxide composites, J. Colloid Interface Sci. 448 (2015) 389–397.
[26] L.M. Zacaroni, Z.M. Magriotis, M.D. Cardoso, W.D. Santiago, J.G. Mendonça, S.S. Vieira, D.L. Nelson, Natural clay and commercial activated charcoal: Properties and application for the removal of copper from cachaça, Food Control 47 (2015) 536–544.
[27] A. Robalds, M. Klavins, L. Dreijalte, Sorption of thallium(I) ions by peat, Water Sci. Technol. 68 (2013) 2208–2213.
[28] J.C. Igwe, A.A. Abia, Adsorption kinetics and intraparticulate diffusivities for bioremediation of Co (II), Fe(II) and Cu (II) ions from waste water using modified and unmodified maize cob, Int. J. Phys. Sci. 2 (2007) 119–127.
[29] N. Asasian, T. Kaghazchi, Comparison of dimethyl disulfide and carbon disulfide in sulfurization of activated carbons for producing mercury adsorbents, Ind. Eng. Chem. Res. 51 (2012) 12046–12057.
[30] A. Hawari, M. Khraisheh, M.A. Al-Ghouti, Characteristics of olive mill solid residue and its application in remediation of Pb^{2+}, Cu^{2+} and Ni^{2+} from aqueous solution: Mechanistic study, Chem. Eng. J. 251 (2014) 329–336.
[31] M. Sarkar, P.K. Acharya, B. Bhattacharya, Modeling the adsorption kinetics of some priority organic pollutants in water from diffusion and activation energy parameters, J. Colloid Interface Sci. 266 (2003) 28–32.
[32] C.J. An, G.H. Huang, Stepwise adsorption of phenanthrene at the fly ash–water interface as affected by solution chemistry: Experimental and modeling studies, Environ. Sci. Technol. 46 (2012) 12742–12750.
[33] I.J. Alinnor, Adsorption of heavy metal ions from aqueous solution by fly ash, Fuel 86 (2007) 853–857.
[34] S.G. Lu, S.Q. Bai, L. Zhu, H.D. Shan, Removal mechanism of phosphate from aqueous solution by fly ash, J. Hazard. Mater. 161 (2009) 95–101.
[35] S. Andini, R. Cioffi, F. Colangelo, F. Montagnaro, L. Santoro, Effect of mechanochemical processing on adsorptive properties of blast furnace slag, J. Environ. Eng. 139 (2013) 1446–1453.
[36] S.R. Kanel, H. Choi, J.Y. Kim, S. Vigneswaran, W.G. Shim, Removal of Arsenic (III) from groundwater using low-cost industrial by-products—Blast furnace slag, Water Qual. Res. J. Can. 41 (2006) 130–139.
[37] D.H. Kim, M.C. Shin, H.D. Choi, C.I. Seo, K. Baek, Removal mechanisms of copper using steel-making slag: Adsorption and precipitation, Desalination 223 (2008) 283–289.
[38] S. Dimitrova, V. Nikolov, D. Mehandjiev, Effect of the heat treatment on the morphology and sorption ability to metal ions of metallurgical slag, J. Mater. Sci. 36 (2001) 2639–2643.
[39] C. Oh, S. Rhee, M. Oh, J. Park, Removal characteristics of As(III) and As(V) from acidic aqueous solution by steel making slag, J. Hazard. Mater. 213–214 (2012) 147–155.
[40] N.Y. Mostafa, S.A.S. El-Hemaly, E.I. Al-Wakeel, S.A. El-Korashy, P.W. Brown, Characterization and evaluation of the hydraulic activity of water-cooled slag and air-cooled slag, Cem. Concr. Res. 31 (2001) 899–904.
[41] R.P. Han, W.H. Zou, Z.P. Zhang, J. Shi, J.J. Yang, Removal of copper(II) and lead(II) from aqueous solution by manganese oxide coated sand, J. Hazard. Mater. 137 (2006) 384–395.
[42] J.M. Duan, B. Su, Removal characteristics of Cd(II) from acidic aqueous solution by modified steel-making slag, Chem. Eng. J. 246 (2014) 160–167.
[43] T.W. Cheng, M.L. Lee, M.S. Ko, T.H. Ueng, S.F. Yang, The heavy metal adsorption characteristics on metakaolin-based geopolymer, Appl. Clay Sci. 56 (2012) 90–96.
[44] Y.J. Xue, S.P. Wu, M. Zhou, Adsorption characterization of Cu(II) from aqueous solution onto basic oxygen furnace slag, Chem. Eng. J. 231 (2013) 355–364.
[45] S.V. Dimitrova, D.R. Mehanjiev, Interaction of blast-furnace slag with heavy metal ions in water solutions, Water Res. 34 (2000) 1957–1961.
[46] J. Zhang, H. Xiao, Y. Zhao, Hemicellulose-based absorbent toward dye: Adsorption equilibrium and kinetics studies, J. Environ. Inf. 24 (2014) 32–38.
[47] H. Freundlich, W. Heller, The Adsorption of cis - and trans -Azobenzene, J. Am. Chem. Soc. 61 (1939) 2228–2230.
[48] M.H. Nasir, R. Nadeem, K. Akhtar, M.A. Hanif, A.M. Khalid, Efficacy of modified distillation sludge of rose (*Rosa centifolia*) petals for lead(II) and zinc(II) removal from aqueous solutions, J. Hazard. Mater. 147 (2007) 1006–1014.
[49] E. Pehlivan, S. Cetin, Sorption of Cr(VI) ions on two Lewatit-anion exchange resins and their quantitative determination using UV-visible spectrophotometer, J. Hazard. Mater. 163 (2009) 448–453.
[50] D.D. Duong, Adsorption Analysis: Equilibrium and Kinetics, Imperial College Press, London, 1998, pp. 291–221.
[51] S.H. Chen, Q.Y. Yue, B.Y. Gao, Q. Li, X. Xu, Removal of Cr(VI) from aqueous solution using modified corn stalks: Characteristic, equilibrium, kinetic and thermodynamic study, Chem. Eng. J. 168 (2011) 909–917.
[52] M. Šljivić, I. Smičiklas, S. Pejanović, I. Plećaš, Comparative study of Cu^{2+} adsorption on a zeolite, a clay and a diatomite from Serbia, Appl. Clay Sci. 43 (2009) 33–40.
[53] H. Zhang, D. Zhao, L. Chen, X.J. Yu, Investigation of Cu(II) adsorption from aqueous solutions by NKF-6 zeolite, Water Sci. Technol. 63 (2011) 395–402.
[54] L.Z. Miao, C. Wang, J. Hou, P.F. Wang, J. Qian, S.S. Dai, Kinetics and equilibrium biosorption of nano-ZnO particles on periphytic biofilm under different environmental conditions, J. Environ. Inf. 23 (2014) 1–9.
[55] P.C. Mishra, R.K. Patel, Removal of lead and zinc ions from water by low cost adsorbents, J. Hazard. Mater. 168 (2009) 319–325.
[56] A.K. Golder, A.N. Samanta, S. Ray, Removal of phosphate from aqueous solutions using calcined metal hydroxides sludge waste generated from electrocoagulation, Sep. Purif. Technol. 52 (2006) 102–109.

[57] M. Şölener, S. Tunali, A.S. Özcan, A. Özcan, T. Gedikbey, Adsorption characteristics of lead(II) ions onto the clay/poly(methoxyethyl)acrylamide (PMEA) composite from aqueous solutions, Desalination 223 (2008) 308–322.
[58] Y. Wang, X.W. Tang, Y.M. Chen, L.T. Zhan, Z.Z. Li, Q. Tang, Adsorption behavior and mechanism of Cd (II) on loess soil from China, J. Hazard. Mater. 172 (2009) 30–37.
[59] S. Vasudevan, J. Lakshmi, G. Sozhan, Optimization of electrocoagulation process for the simultaneous removal of mercury, lead, and nickel from contaminated water, Environ. Sci. Pollut. Res. 19 (2012) 2734–2744.
[60] S. Azizian, Kinetic models of sorption: A theoretical analysis, J. Colloid Interface Sci. 276 (2004) 47–52.
[61] M.R. Mehrasbi, Z. Farahmandkia, B. Taghibeigloo, A. Taromi, Adsorption of lead and cadmium from aqueous solution by using almond shells, Water, Air, Soil Pollut. 199 (2009) 343–351.
[62] M. Rafatullah, O. Sulaiman, R. Hashim, A. Ahmad, Adsorption of copper (II), chromium (III), nickel (II) and lead (II) ions from aqueous solutions by meranti sawdust, J. Hazard. Mater. 170 (2009) 969–977.
[63] X.L. Li, Y.F. Li, Z.F. Ye, Preparation of macroporous bead adsorbents based on poly(vinyl alcohol)/chitosan and their adsorption properties for heavy metals from aqueous solution, Chem. Eng. J. 178 (2011) 60–68.
[64] Y. Zhang, Y.F. Li, L.Q. Yang, X.J. Ma, L.Y. Wang, Z.F. Ye, Characterization and adsorption mechanism of Zn^{2+} removal by PVA/EDTA resin in polluted water, J. Hazard. Mater. 178 (2010) 1046–1054.
[65] C.J. Chang, L. Tseng, T.S. Lin, W.J. Wang, T.C. Lee, Recycling of modified MSWI ash-mix slag and CMP sludge as a cement substitute and its optimal composition, Indian J. Eng. Mater. S. 19 (2012) 31–40.